Engineering a Functional Blue-Wavelength-Shifted Rhodopsin Mutant†

Jay M. Janz and David L. Farrens*

Department of Biochemistry and Molecular Biology, Oregon Health Sciences University, 3181 Southwest Sam Jackson Park Drive, Portland, Oregon 97201-3098

Received December 27, 2000; Revised Manuscript Received March 24, 2001

ABSTRACT: We report an effort to engineer a functional, maximally blue-wavelength-shifted version of rhodopsin. Toward this goal, we first constructed and assayed a number of previously described mutations in the retinal binding pocket of rhodopsin, G90S, E122D, A292S, and A295S. Of these mutants, we found that only mutants E122D and A292S were like the wild type (WT). In contrast, mutant G90S exhibited a perturbed photobleaching spectrum, and mutant A295S exhibited decreased ability to activate transducin. We also identified and characterized a new blue-wavelength-shifting mutation (at site T118), a residue conserved in most opsin proteins. Interestingly, although residue T118 contacts the critically important C_9-methyl group of the retinal chromophore, the T118A mutant exhibited no significant perturbation other than the blue-wavelength shift. In analyzing these mutants, we found that although several mutants exhibited different rates of retinal release, the activation energies of the retinal release were all ∼20 kcal/mol, almost identical to the value found for WT rhodopsin. These latter results support the theory that chemical hydrolysis of the Schiff base is the rate-limiting step of the retinal release pathway. A combination of the functional blue-wavelength-shifting mutations was then used to generate a triple mutant (T118A/E122D/A292S) which exhibited a large blue-wavelength shift (absorption $\lambda_{max} = 453$ nm) while exhibiting minimal functional perturbation. Mutant T118A/E122D/A292S thus offers the possibility of a rhodopsin protein that can be worked with and studied using more ambient lighting conditions, and facilitates further study by fluorescence spectroscopy.

Trichromatic color vision is mediated by three types of cone cells, which contain opsin pigments that absorb maximally at three different wavelengths: blue (414 nm), green (533 nm), and red (560 nm) (*1*−*3*). In contrast, dim light vision is mediated by the rod photoreceptor rhodopsin that absorbs maximally at 500 nm. Rhodopsin is the only G-protein-coupled receptor (GPCR)[1] with a crystal structure and is arguably the best-characterized member of this large and important family of sensory proteins (for reviews, see refs *4*−*6*). All of these visual pigments are thought to share a similar, general structure of seven TM helices (with a chromophore, 11-*cis*-retinal, attached to a lysine residue) (*7*, *8*). The resulting color absorption by the different opsins is due to "spectral tuning" (i.e., controlling the λ_{max} of rhodopsin) through interactions of amino acids lining the chromophore binding pocket with the protonated Schiff base (PSB) (*9*, *10*).

The mechanism of spectral tuning in opsin proteins is being elucidated by the efforts of several laboratories through a combination of mutagenesis, absorption spectroscopy, and Raman spectroscopy techniques (*11*−*17*). One of these studies has shown that substitutions of nine rhodopsin amino acids can account for ∼80% of the opsin shift between the blue cone pigment and rhodopsin (*10*), and suggested that a blue-wavelength shift may be induced by dipolar substitutions through long-range electrostatic effects on the change in dipole moment of the photoexcited chromophore (*10*). However, complementary experiments carried out on the human blue cone pigment indicate that although mutagenesis studies on bovine rhodopsin serve well as predictive models of spectral tuning near the ring portion of the retinal, mutations near the Schiff base do not (*1*). In general, although these informative studies have gone far to shed light on understanding the process of spectral tuning, little work investigating the functional effects of introducing blue-wavelength-shifting mutations into bovine rhodopsin has been carried out.

The goal of this paper is to use some of the previously identified blue-wavelength-shifting mutations to engineer a maximally blue-wavelength-shifted rhodopsin that retains functionality (i.e., normal stability of the MII state and ability to activate the G-protein transducin). In the process of these studies, we also identified and characterized a new blue-wavelength-shifting mutation at site T118, a residue conserved in most opsin proteins and found to be in contact with the C_9-methyl group of the retinal chromophore (*18*). In addition, while characterizing these mutants, we found

† This work was supported by Grants EY12095-01 to D.L.F. and T32-EY07123-09 to J.M.J. from the National Eye Institute, and by funds from the N. L. Tartar Trust Fellowship to J.M.J. from the Medical Research Fund of Oregon.

* To whom correspondence should be addressed. Telephone: (503) 494-0583. Fax: (503) 494-8393. E-mail: farrensd@ohsu.edu.

[1] Abbreviations: DM, *n*-dodecyl *β*-maltoside; DS, dark state rhodopsin; E_a, energy of activation; EDTA, ethylenediaminetetraacetic acid; G-protein, guanine nucleotide-binding regulatory protein; GPCR, G-protein-coupled receptor; $G_{T\alpha}$, α-subunit of transducin; GTPγS, gaunosine 5′-3-*O*-(thio)triphosphate; λ_{max}, absorption maxima; MES, 2-(*N*-morpholino)ethanesulfonic acid monohydrate; MI, metarhodopsin I; MII, metarhodopsin II; T/E/A, T118A/E122D/A292S mutant; TM, transmembrane; Tris, 2-amino-2-(hydroxymethyl)-1,3-propanediol; PSB, protonated Schiff base; WT, wild-type COS-1-expressed bovine rhodopsin.

10.1021/bi002937i CCC: $20.00
Published on Web 05/22/2001

evidence supporting the conclusion that the rate-limiting step in retinal release is the chemical event of Schiff base hydrolysis.

MATERIALS AND METHODS

Materials. All buffers and chemicals were purchased from either Fisher or Sigma except where noted below. Protease inhibitor cocktail tablets and GTPγS were purchased from Boehringer Mannheim. Dodecyl maltoside (DM) was purchased from Anatrace (Maumee, OH), and GBX red filters were from Eastman Kodak Corp. Polystyrene columns (2 mL bed volume) were purchased from Pierce. Frozen bovine retinas were from J. A. Lawson Co. (Lincoln, NE). Transducin was purified from rod outer segments as previously described (*19*). Restriction endonucleases were from New England Biolabs (Beaverly, MA). 11-*cis*-Retinal was a generous gift from R. Crouch (Medical University of South Carolina and National Eye Institute). The 1D4 antibody was purchased from the National Cell Culture Center (Minneapolis, MN). The nonapeptide corresponding to the C-terminus of rhodopsin was acquired from the Emory University Microchemical Facility (Atlanta, GA). Cuvettes were purchased from Uvonics (Plainview, NY). Band-pass filters and long-pass filters were purchased from Oriel (Stratford, CT).

Buffers. The definitions of the buffers used in this report are as follows: PBSSC [0.137 M NaCl, 2.7 mM KCl, 1.5 mM KH_2PO_4, and 8 mM Na_2HPO_4 (pH 7.2)], buffer A [5 mM Tris-HCl and 2 mM EDTA (pH 7.4)], buffer B [1% DM and PBSSC (pH 7.2)], buffer C [2 mM ATP, 0.1% DM, 1 M NaCl, and 2 mM $MgCl_2$ (pH 7.2)], buffer D [0.05% DM and PBSSC (pH 7.0)], and buffer E [0.05% DM and MES (pH 6.0)].

Construction and Expression of Rhodopsin Mutants. Site-directed mutagenesis was performed as described previously in the PMT4 plasmid (*20*, *21*). Specifically, mutant T118A was generated by replacement of the *Xho*I−*Pvu*I fragment in the synthetic bovine rhodopsin gene with synthetic oligonucleotide duplexes containing the corresponding sequence GCC for ACC to generate T118A. Mutants A292S and A295S were generated in a similar manner by replacing the *Apa*I−*Aat*II fragment containing the corresponding sequence TCT with GCT at each site. Overlap extension PCR was used to generate *Eco*RI and *Not*I fragments containing either the G90S or E122D mutation (*22*). The sequences for the primers were as follows: 5′GTCTTCGGTTCGTTCACCACCACCCTC3′ for G90S and 5′GGGCGGTGACATTGCACTGTGGTCTCT3′ for E122D. These PCR fragments were then subcloned into PMT4 using *Bcl*I−*Xho*I restriction sites for G90S and *Xho*I−*Sfi*I sites for E122D. All mutations were confirmed by the dideoxynucleotide sequencing method. The mutant rhodopsin proteins were transiently expressed in COS-1 cells using the DEAE-dextran method, and cells were harvested 52−56 h after transfection (*23*, *24*).

Purification of Rhodopsin Mutants. Prior to mutant purification, the cell membranes were prepared as follows. Briefly, five 15 cm plates of transfected COS-1 cells were washed twice with 7 mL of cold PBSSC buffer, pelleted, and subsequently lysed in 10 mL of cold buffer A containing 0.5 mM PMSF in the presence of protease inhibitors. Cells were subsequently vortexed and spun at 45000*g* to pellet cell membranes. The remaining steps in the procedure were carried out under dark room conditions under filtered red light. The membranes were resuspended in 10 mL of cold PBSSC (pH 6.5) and regenerated with 11-*cis*-retinal (10 μL of a 10 mM stock) at 4 °C for 1 h as previously described (*25*), and then an additional 5 μL of 11-*cis*-retinal was added and regeneration allowed to proceed for an additional 1 h. The purification of the rhodopsin mutants proceeded essentially as the original procedure (*23*) except small polystyrene columns were used (*26*). Rhodopsin-containing membranes were solubilized in 5 mL of buffer B containing 0.5 mM PMSF at 4 °C for 1 h, and then centrifuged at 45000*g*. The supernatant was mixed with 200 μL of 1D4 antibody−Sepharose beads (binding capacity $\sim$ 1 μg of rhodopsin/μg of resin) in buffer C containing 0.5 mM PMSF and mutated at 4 °C for 4−5 h. The slurry was subsequently transferred to polystyrene columns and washed once with 50 mL of buffer D followed by a 40 mL wash with buffer E by gravity filtration. During the last 5 mL of the second wash, a 27 gauge 0.5 in. needle was attached to the column to decrease the flow rate. Samples were eluted in 300 μL fractions of buffer E containing 200 μM nonapeptide corresponding to the 1D4 antibody epitope (the last nine amino acids of the C-terminus of rhodopsin). A spectrum of each elution fraction was recorded using a Shimadzu UV-1601 spectrophotometer (described below), and the purified samples were snap frozen in liquid N_2 and stored at −80 °C.

UV−Vis Absorption Spectroscopy. All UV−vis absorption spectra were recorded with a Shimadzu UV-1601 spectrophotometer at 20 °C using a bandwidth of 2 nm, a response time of 1 s, and a scan speed of 240 nm/min unless otherwise noted. For calculations, a molar extinction coefficient value (λ_{500}) for WT rhodopsin was taken to be 40 600 M^{-1} cm^{-1} (*27*). The samples were photobleached in buffer E by illumination for 30 s (at a 6 Hz flash rate) with a Machine Vision Strobe light source (EG&G) equipped with a wavelength > 490 nm long-pass filter. This light treatment was found to be adequate for full conversion of samples, as 5 s was sufficient for full bleaching of WT rhodopsin. The blue-wavelength-shifted mutants were bleached using a wavelength > 470 nm long-pass filter to ensure full bleaching. The presence of a PSB in the MII state for each mutant was verified by adding H_2SO_4 to a pH of 1.9 and immediately following photobleaching measuring the absorbance spectrum (within 1 min) to look for the presence of a spectral species at 440 nm (representative of a PSB linkage that is present in the acid) (*28*). Rhodopsin mutants that exhibited abnormal bleaching behavior were studied further as a function of time after irradiation as described previously (*29*). Extinction coefficients were determined as previously described in buffer E at 15 °C (*30*).

Measurement of the Rate of Retinal Release and/or MII Decay by Fluorescence Spectroscopy. The MII stability was assessed by measuring the time course of retinal release after MII on a Photon Technologies QM-1 steady state fluorescence spectrophotometer (*31*). Each measurement was carried out using 80 μL of a 0.25 μM mutant sample in buffer E, and the sample temperatures were maintained using a water-jacketed cuvette holder. After the samples had been photobleached to the MII state (see above), the retinal release measurements were carried out at the appropriate temperature by exciting the sample for 3 s (excitation wavelength = 295

nm, $^1/_4$ nm bandwidth slit setting) and then blocking the excitation beam for 42 s, to avoid photobleaching the samples. Tryptophan fluorescence emission was monitored at 330 nm (12-nm bandwidth slit setting), and this cycle was repeated for 90 min during each measurement. Results were analyzed manually to determine the $t_{1/2}$ values. Series of MII decay rates were obtained at 13, 20, 27, and 33 °C, and the rates were applied to the Arrhenius equation [$k = Ae^{-E_a/(RT)}$] to determine the activation energy (E_a) of each mutant rhodopsin.

Determination of Transducin ($G_{T\alpha}$) Activation Rates. Activation of $G_{T\alpha}$ by rhodopsin was monitored using fluorescence spectroscopy at 20 °C as described previously (*21*, *32*, *33*). The excitation wavelength was 295 nm (2 nm bandwidth), and fluorescence emission was monitored at 340 nm (12 nm bandwidth). G_T was added (final concentration of 250 nM) to the reaction mixture containing 10 mM Tris (pH 7.2), 2 mM $MgCl_2$, 100 mM NaCl, 1 mM DTT, and 0.01% DM. The solution was stirred for 300 s to establish a baseline. Photobleached mutant rhodopsin (see above) was then added to the mixture to a final concentration of 5 nM and the mixture allowed to stir for 300 s to equilibrate. GTPγS was added to the reaction mixture to a final concentration of 5 μM, and the increase in fluorescence was followed for an additional 2000 s. To calculate the activation rates, the slopes of the initial fluorescence increase after GTPγS addition were determined through the data points covering the first 60 s.

RESULTS

Sites Selected for Mutagenesis in Bovine Rhodopsin. Amino acids G90, E122, A292, and A295 were selected for mutagenesis on the basis of previous work indicating that substitutions at these sites confer a hypsochromatic shift (*10*, *32*, *34*−*36*). While other blue-wavelength-shifted mutants have been previously reported (for example, W265 and F268), we did not pursue mutations of these residues because substitution at these sites either perturbs the ability of opsin to bind retinal or results in a nonfunctional mutant pigment (*35*, *37*). The rationale for studying the amino acids we chose is as follows. A serine residue at the equivalent of position 292 causes the blue-wavelength shift in the dolphin long-wavelength sensitive cone photopigment (*36*). Mutations G90S, E122D, and A295S were previously observed to confer blue shifts in λ_{max} when introduced into bovine rhodopsin (*10*, *35*). We investigated a previously unidentified site, position T118, because it is conserved in most opsins and is located approximately one turn above the counterion (E113) and thus might be expected to perturb the location of the counterion, resulting in a blue-wavelength shift (*38*).

Spectral Characterization of Rhodopsin Mutants. In general, yields of purified mutant protein were comparable to that of WT rhodopsin (~10 μg/15 cm plate). All mutants formed characteristic rhodopsin-like chromophores after purification with spectral ratios [$A_{280}/A(\lambda_{max})$] between 1.6 and 1.8 (Figure 2). All of the mutants (except G90S) exhibited normal bleaching behavior with respect to formation of a $\lambda_{max} = 380$ nm species, characteristic of the MII intermediate (*7*). Acidification of these photobleached samples generated a $\lambda_{max} \sim 440$ nm species, indicating the presence of a protonated retinal Schiff base (*28*). An example of normal photobleaching behavior is shown for mutant T118A (Figure 3A), and these results are compiled in Table 1. In contrast, mutant G90S, while being capable of forming both a MII species and a PSB, exhibited abnormal bleaching behavior (Figure 3B). Following illumination, a residual species with a λ_{max} of ~480 nm persisted in the G90S mutant. This species was followed as a function of time after irradiation, and even 10 h after illumination, a residual amount of the $\lambda_{max} \sim 480$ nm species could be detected (Figure 3B). To test whether this ~480 nm species is representative of the MI photointermediate, bleaching was performed in the presence of transducin. Transducin binding should shift the MI−MII equilibrium to the MII state (*39*−*41*). The presence of transducin (1 μM) was observed to have no effect on G90S bleaching behavior (data not shown), suggesting the ~480 nm species in G90S is not a normal MI-like photoproduct.

Retinal Release Rates of Wavelength-Shifted Single Mutants. The rate of retinal release from the MII state was measured using a fluorescence-based assay (*31*) at 20 °C. Under the conditions used for bleaching, the $t_{1/2}$ for retinal release for WT rhodopsin buffer E was 15 min. The corresponding $t_{1/2}$ values for the wavelength-shifted single mutants ranged from 4.8 to 26 min (Table 1). Only mutant A295S exhibited a strikingly accelerated retinal release rate ($t_{1/2} = 4.8$ min). In contrast, mutant E112D exhibited a slower rate of retinal release ($t_{1/2} = 26$ min). The observed 2-fold decrease in the level of retinal release for E122D with respect to WT is in agreement with the slowed MII decay rate for this mutant obtained by low-temperature time-resolved spectroscopy (*42*). The values for each of the mutants are compiled in Table 1.

Transducin Activation by Wavelength-Shifted Mutants. The blue-wavelength-shifted mutants were next tested for their ability to activate transducin using a fluorescence-based assay which measures the increase in tryptophan fluorescence of the $G_{T\alpha}$−GTPγS species (*33*, *43*). The results are shown in Figure 4B as initial rates of fluorescence increase relative to WT rhodopsin. An example representative of the data that were collected is shown in Figure 4A. Mutants G90S, T118A, E122D, and A292S exhibit rates of fluorescence increase that are similar to that of WT rhodopsin. Mutant A295S was much less able to activate transducin as judged from its initial rate of fluorescence increase. These results are summarized in Table 2.

Activation Energy for Meta II Decay Measured by Fluorescence Increase. The rate of fluorescence increase from photobleached WT rhodopsin and blue-wavelength-shifted mutants was measured in buffer E at four different temperatures (13, 20, 27, and 33 °C). The rate of fluorescence increase in all cases was temperature-dependent, and Arrhenius plots of these measurements indicate a temperature-dependent linear relationship for all mutants (Figure 5). From these plots, an activation energy (E_a) of 20.1 kcal/mol was obtained for WT rhodopsin, in good agreement with the previously reported value of 20.2 kcal/mol (*31*). Interestingly, although several of the blue-wavelength-shifted mutants exhibited different rates of retinal release (see Table 1), an Arrhenius plot of the retinal release rates measured at different temperatures showed nearly equal E_a values for the mutants (Figure 5 and Table 2). For example, mutants G90S, T118A, and A292S had retinal release rates slightly faster

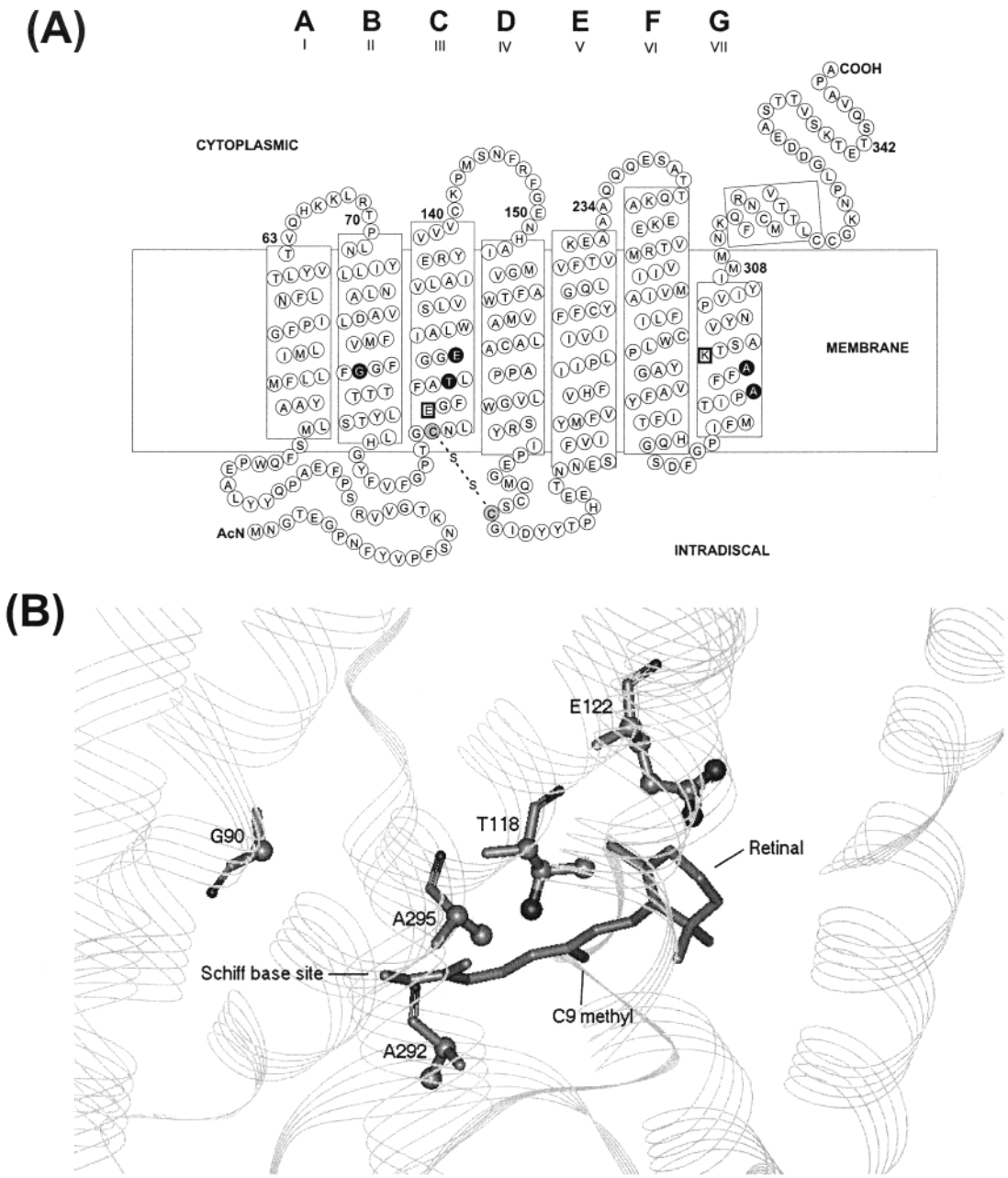

FIGURE 1: Models of bovine rhodopsin indicating sites for introducing blue-wavelength-shifting mutations. (A) Suggested two-dimensional model of rhodopsin. Individual amino acids mutated in this study are shown in bold, and cysteine residues involved in a disulfide bond are shaded gray. K296, the retinal Schiff base attachment site, and E113, the counterion, are boxed. The cytoplasmic side is at the top in this rendition, with labels A−G referring to the TM helices below. (B) Three-dimensional model of the retinal binding pocket of rhodopsin adapted from the bovine opsin crystal structure (*18*). Sites mutated in this study are shown with respect to the retinal chromophore.

than that of WT at any given temperature, yet the Arrhenius plot of these measurements yielded E_a values that were very similar for each (Table 2). The most extreme differences in retinal release rates were found for mutant A295S (exhibited a 3-fold increased rate of retinal release; 4.5 min) and mutant E122D (exhibited a ~2-fold decreased rate of retinal release; 26 min).

Construction of a Substantially Blue-Wavelength-Shifted Mutant with Minimal Spectral Perturbation. The spectral characterization of rhodopsin blue-wavelength-shifted point mutants indicated two of the mutations (G90S and A295S) are structurally and/or functionally perturbing when introduced into bovine rhodopsin (see Figures 3B and 4B and Tables 1 and 2). G90S exhibits abnormal photobleaching properties, whereas mutant A295S exhibits an accelerated MII decay rate, suggesting it is not stable. In contrast, the other three blue-wavelength-shifted mutants (T118A, E122D, and A292S) exhibit behavior more like that of the wild type, and thus were subsequently combined into a single mutant and further characterized, as described below.

Spectral Characterization of Mutant T118A/E122D/A292S. The triple point mutant T118A/E122D/A292S was expressed at levels similar to that of WT (~10 μg/15 cm plate) and formed a rhodopsin-like chromophore with a spectral ratio [$A_{280}/A(\lambda_{max})$] of 1.7 (Table 3). Mutant T118A/E122D/A292S exhibits a 47 nm blue shift relative to WT rhodopsin with a λ_{max} at 453 nm (Table 3 and Figure 6). The slight narrowing of the spectral curve can be attributed to the E122D mutation

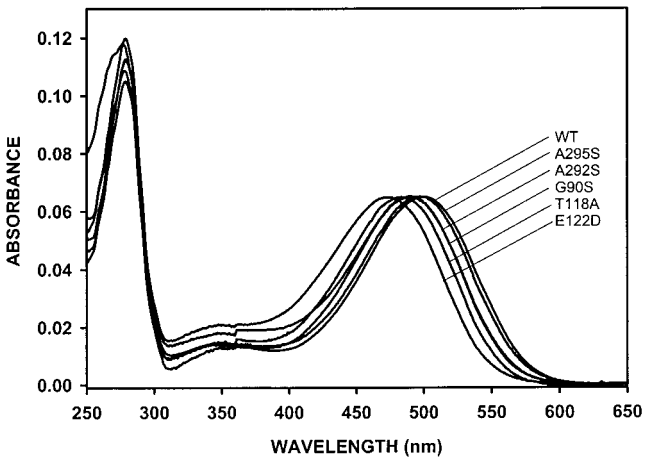

FIGURE 2: UV−vis absorption spectra of WT and mutant rhodopsin pigments in the dark state. The respective blue shifts in λ_{max} are indicated. The spectra were recorded in buffer E at 20 °C. For display purposes, the WT and A292S spectra were divided by 1.4 to allow for comparison with the other spectra.

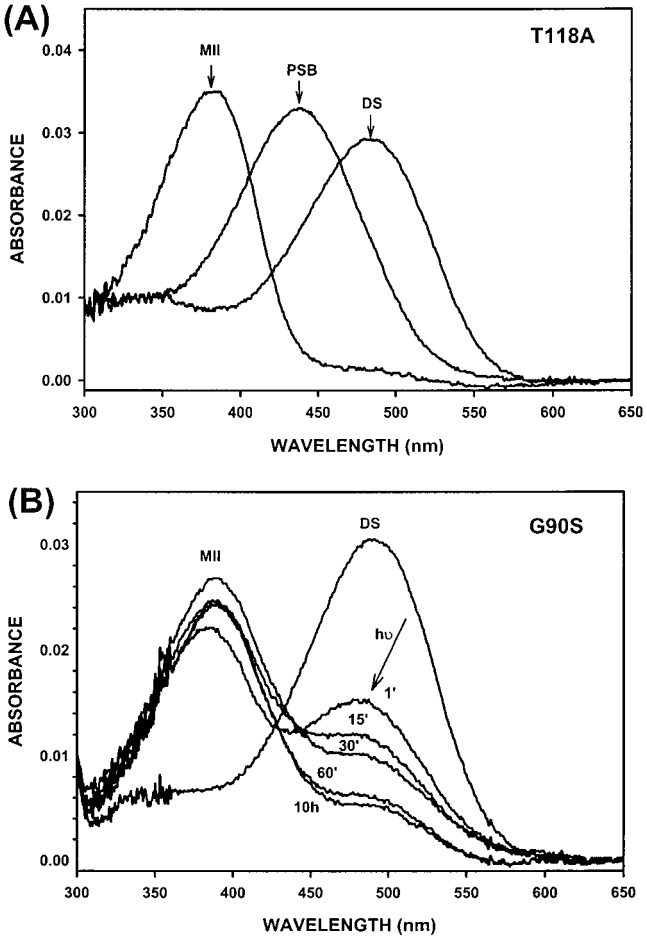

FIGURE 3: UV−vis spectral properties of select blue-wavelength-shifted rhodopsin mutants. (A) Photobleaching properties of T118A. DS, dark state; MII, meta II state; PSB, protonated Schiff base (at pH 1.9). (B) Photobleaching properties of G90S. Following illumination (λ > 470 nm) for 30 s, a residual species remains with a λ_{max} of ~480 nm. This species was followed as a function of time as indicated.

(*35*). The effects that individual mutations have upon λ_{max} of the pigment appear to be additive (Tables 1 and 3). Photobleaching analysis indicates that the engineered opsin is capable of forming a MII species (λ_{max} = 380 nm), and upon acidification forms a PSB (λ_{max} = 440 nm) (Figure 6). The rate of retinal release of the engineered opsin exhibits a $t_{1/2}$ value of 11.1 min. The spectral characteristics of T118A/E122D/A292S are compiled in Table 3. Additionally, T118A/E122D/A292S is functionally active. The engineered opsin is able to activate transducin with a relative initial rate of activation that is ~50% of that of WT rhodopsin (Table 3).

Table 1: Functional Characterization of Wavelength-Shifted Single-Point Mutants (Spectral Ratio, Absorption Maxima, Absorption Shift, Extinction Coefficient, and $t_{1/2}$ of Retinal Release Rates)

	$A_{280}/A(\lambda_{max})$	λ_{max}	λ shift (nm)	ϵ (M^{-1} cm^{-1})[a]	MII decay $t_{1/2}$ (min)[b]
WT	1.8	500	−	40 600[c]	15
G90S	1.8	487[d]	13	39 000	10.3
T118A	1.8	484	16	41 000	10.6
E122D	1.6	477[e]	23	45 000[f]	26
A292S	1.7	489.5[d]	9.5	40 500	10.5
A295S	1.6	498	2	45 000	4.8

[a] Extinction coefficients determined in buffer E at 15 °C; for further details, see Materials and Methods. [b] MII decay assays performed in buffer E at 20 °C as described in Materials and Methods. [c] The extinction coefficient for WT was assumed to be 40 600 M^{-1} cm^{-1} (*27*). [d] λ_{max} similar to that from ref *35*. [e] λ_{max} similar to that from ref *10*. [f] Extinction coefficient similar to that from ref *30*.

DISCUSSION

In this paper, we systematically investigated the structural and functional consequences of introducing blue-wavelength-shifting mutations into the retinal binding pocket of bovine rhodopsin. Our goal was to develop a mutant rhodopsin that exhibits maximal blue-wavelength shift yet remains stable in terms of structure and function for future use in biophysical studies. To achieve this goal, we engineered a series of five point mutations based on their ability to confer a blue-wavelength shift. Amino acids at positions 90, 122, 292, and 295 were chosen for mutation since these residues had been shown in earlier studies to affect the λ_{max} of the mutant pigment (*10*, *32*, *34*, *35*). In our hands, all of these mutants exhibited expression levels similar to that of WT rhodopsin (~10 μg/15 cm plate) and could be purified to homogeneity forming rhodopsin-like chromophores, with spectral ratios [$A_{280}/A(\lambda_{max})$] between 1.6 and 1.8 (Figure 2 and Table 1). In the work presented here, we also characterize a mutation at a new position, T118, where a threonine exists in almost all known opsin proteins. We find that a T118A mutation affects the λ_{max} of the mutant pigment (Figure 3A). The effects of the various wavelength-shifting mutations are discussed further below.

Photobleaching Behavior of Blue-Wavelength-Shifted Mutants. All of the blue-wavelength-shifted mutants exhibited normal photobleaching behavior (for example, see Figure 3A), except for mutant G90S, which exhibited a slow decaying species at ~480 nm (Figure 3B). Note also that a mutation at G90 (G90D) previously has been shown to exhibit abnormalities in photobleaching behavior (*34*, *44*). Since the λ_{max} of the residual decay species is ~480 nm, it is possible that this mutation disrupts the MI−MII equilibrium (*45*). To see if the species represents a transient MI-like species, we bleached it in the presence of transducin (1 μM), but no absorbance shift was observed, arguing against the residual ~480 nm species being a transitional MI

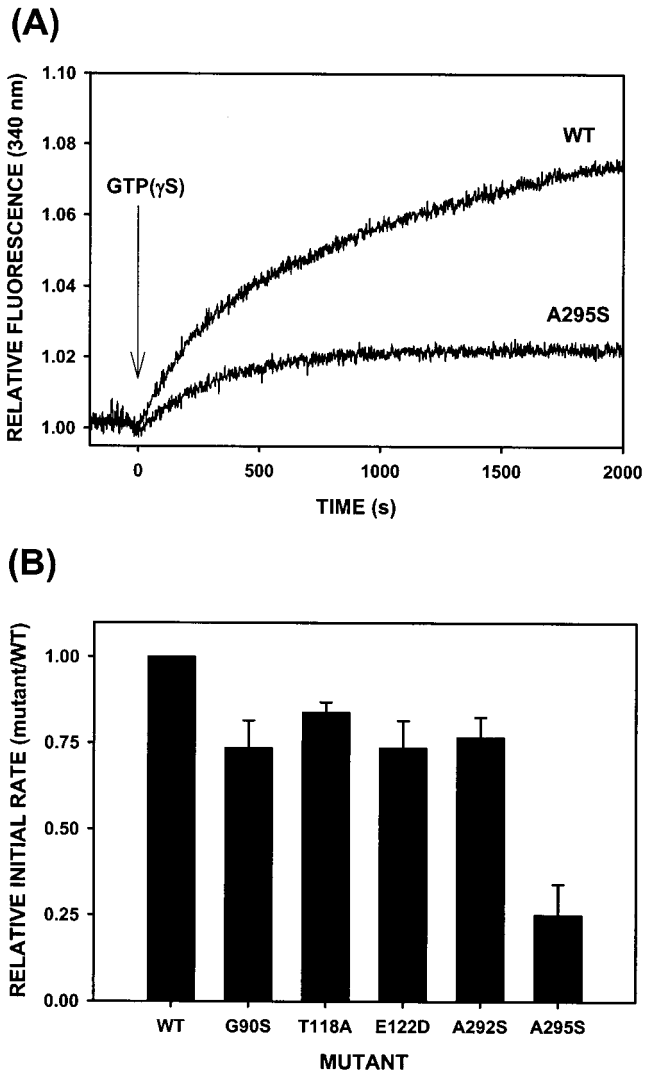

FIGURE 4: Transducin activation by blue-wavelength-shifted rhodopsin mutants. (A) Example of transducin activation as assessed by the fluorescence assay. The assay directly monitors transducin activation by measuring the increase in $G_{T\alpha}$ tryptophan fluorescence that occurs upon formation of the $G_{T\alpha}$−GTPγS complex when GTPγS is added (arrow). For assay conditions and further details, see Materials and Methods. (B) Comparison of the initial rates of transducin activation by wavelength-shifted rhodopsin mutants. The rate in the first minute after GTPγS addition relative to wild-type rhodopsin is shown for each mutant.

Table 2: Relative Transducin Activation Rates and Activation Parameters of Retinal Release[a]

	relative level of transducin activation	E_a (kcal/mol)
WT	1.00	20.1
G90S	0.74	19.6
T118A	0.84	19.7
E122D	0.76	16.3
A292S	0.77	19.2
A295S	0.25	21.1

[a] All experiments performed in buffer E as described in Materials and Methods.

intermediate (data not shown). Because the G90S mutant is capable of activating transducin upon light activation (see Figure 4B), and forms a PSB upon acidification (data not shown), we surmise that the ~480 nm species represents an active, MII-like intermediate containing a PSB, as was

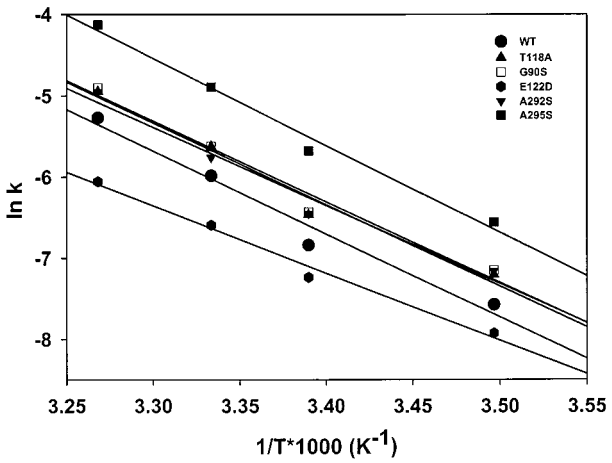

FIGURE 5: Arrhenius plot of the retinal release rates from photobleached WT and mutant rhodopsins. The rate constants were obtained from traces of the retinal release assay (see Materials and Methods) performed in buffer E, with temperatures ranging from 13 to 33 °C. The activation energy (E_a) of this process for WT and all mutants is given in Table 2.

suggested for the G90D mutant (*34*, *44*). Additionally, G90S exhibits a slightly faster rate of retinal release than WT (~50% faster, Table 1) but a rate not as fast as that reported for G90D which (by a different assay) was found to have a $t_{1/2}$ PSB decay that was ~25% that of WT (*44*). Interestingly, the recently determined crystal structure of WT rhodopsin models the G90 residue more than 4.5 Å away from the Schiff base attachment site (*18*), too far away for direct hydrogen bonding interactions. This fact suggests other factors contribute to the mechanism of wavelength shifting by mutations at the G90 site. One possibility is that mutations at this site disrupt bridging water molecules, which could also account for the perturbed photobleaching and activation properties exhibited by this mutant. Indeed, previous results of investigating mechanisms of spectral tuning in the human blue cone pigment have shown that although substitutions in the ring portion of the retinal binding pocket of bovine rhodopsin can be predictive on the basis of the analogous residues in the human blue cone pigment, mutations near the Schiff base are not necessarily complementary (*1*).

Transducin Activation. With the exception of the A295S mutant, most of the mutants that were tested were able to activate transducin with initial rates similar to that of WT (Figure 4B). The fact that mutant T118A was able to activate transducin so well was surprising; the recently determined crystal structure of bovine rhodopsin reveals that this site is found to contact the C_9-methyl group of the retinal chromophore (*18*). The local steric interaction between the retinal C_9-methyl with amino acids in the chromophore-binding pocket has led to the "steric trigger" model of rhodopsin activation (*46*). Experimental support for this model demonstrates that regeneration of opsin with a 9-demethylretinal analogue results in a reduced ability of the artificial pigment to activate transducin (*47*). Furthermore, the C_9-methyl group is proposed to act as a scaffold for opsin to adjust key donor and acceptor side chains for the proton transfer reactions that stabilize the active signaling state (*48*), and is thought to impact the MI−MII equilibrium upon photoactivation (*45*).

Thus, we expected that a T118A mutation might be functionally similar to an artificial pigment regenerated with

Table 3: Functional Properties of Mutant T118A/E122D/A292S in Comparison with WT Rhodopsin (Spectral Ratio, Absorption Maxima, Extinction Coefficient, $t_{1/2}$ of Retinal Release Rates, Relative Transducin Activation Rates, and Activation Parameters of Retinal Release)

	$A_{280}/A(\lambda_{max})$	λ_{max} (nm)	ϵ (M^{-1} cm^{-1})[a]	MII decay $t_{1/2}$ (min)	relative rate of G_T activation	E_a of retinal release (kcal/mol)
WT	1.8	500	40 600[b]	15	1.0	20.1
T/E/A	1.7	453	40 000	10	0.51	21.1

[a] Extinction coefficients determined in buffer E at 15 °C; for further details, see Materials and Methods. All values were rounded to the nearest 500 M^{-1} cm^{-1}. [b] The extinction coefficient for WT was assumed to be 40 600 M^{-1} cm^{-1} (*27*).

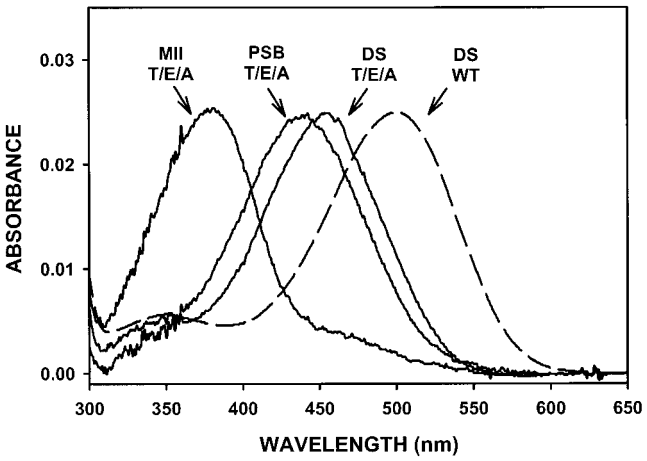

FIGURE 6: UV−vis spectral properties of rhodopsin mutant T118A/E122D/A292S (T/E/A) relative to those of WT. Mutant T/E/A exhibits a 47 nm blue-wavelength shift relative to WT in the dark state (DS). Following illumination (λ > 470 nm) for 30 s, T/E/A adopts the MII state. Upon acidification (to pH 1.9), the absorbance maximum of the T/E/A MII species changes to 440 nm, that of a protonated Schiff base (PSB). The dark state (DS) spectrum of a WT sample (dashed line) is included for comparison purposes.

9-demethylretinal; however, this was not observed. To our surprise, while the T118A mutation clearly affects the spectral tuning of the mutant pigment, it essentially conferred no other structural or functional perturbations that we could detect. However, mutations at this site may confer constitutive activity of the receptor in the dark state, and future experiments should address this possibility.

The wavelength shift caused by the T118A mutation may be due to perturbation of the secondary structure of TM helix 3, and potentially causes the repositioning of the E113 counterion, or water molecules within the chromophore binding pocket and/or neighboring amino acids, leading to the observed blue-wavelength shift (*10*, *49*, *50*). Further, it is also possible that the methyl group of the alanine substitutions is sufficient to interact with the C_9-methyl of 11-*cis*-retinal, thus accounting for WT-like function, or that water molecules may compensate for the lost OH hydrogen bond interactions as well as fill the steric void caused by the alanine mutation. While we are not sure of the precise mechanism of the blue shift caused by T118A, future studies using a combination of site-directed mutagenesis at this residue in conjunction with resonance Raman and/or retinal analogues may prove helpful in understanding the cause of the blue shift in this region. Our results do not resolve the issue of the role the C_9-methyl group plays in receptor activation, nor the potential roles for amino acids that interact with this important moiety. However, our results suggest that future experiments might incorporate sterically small residues such as glycine or bulky amino acid side chain groups at position 118 to test the proposed steric trigger mechanism. Additionally, a serine substitution at this site may provide insight into the role of the hydroxyl residue at position 118 in signal transduction.

The A295S mutant had a 4-fold lower initial rate of transducin activation than WT (Figure 4). Our interpretation of this result is as follows. The A295S mutant exhibited rapid retinal release rates, approximately 3-fold faster at 20 °C than that of WT (Table 1). During bleaching of the samples (prior to incubation with the transducin mixture in the cuvette), the faster initial retinal release rate of A295S reduces the population that can activate transducin, leading to the decreased rate of transducin activation in the G-protein activation assay. Taking into account the parameters of the assay and the MII decay rate for A295S (4.8 min), we calculate that there is less than half of the active sample present during the assay (data not shown). The rapid A295S MII decay might be due to the fact that it is positioned adjacent to the retinal Schiff base attachment site (K296). This may be important because one model of rhodopsin retinal Schiff base hydrolysis involves a tetrahedral carbinolamine intermediate in the MI−MII transition preceding Schiff base hydrolysis (*51*). Thus, it is possible that the serine substitution at A295 acts either to stabilize this intermediate or to provide general acid catalysis (by activating a water molecule involved in the attack) to this mechanism. Either scenario would serve to expedite the Schiff base hydrolysis reaction.

Thermodynamic Parameters and Activation Energies of Retinal Release. The rate-limiting step for retinal release from the chromophore binding pocket may be either (1) the chemical process of Schiff base hydrolysis or (2) unfavorable steric interactions between all-*trans*-retinal and amino acids forming the binding pocket (shown here in brackets).

$$\text{DS} \overset{h\nu}{\longleftrightarrow} [\text{MII}-\text{PSB}] \leftrightarrow [\text{opsin}-\text{retinal}] \rightarrow \text{opsin} + \text{free retinal}$$

In this scheme, rhodopsin forms MII (indicated by the presence of a PSB) following illumination. The MII state next converts to opsin with all-*trans*-retinal still in the binding pocket. In the final stage (which is irreversible), free retinal leaves the chromophore-binding pocket. Although some of the retinal release rates differ from that of WT, the largest difference was only a ~3-fold rate increase. While we cannot unequivocally rule out the possibility that these residues play a direct role, these findings suggest that none of the residues described in this work play a direct catalytic role in the Schiff base hydrolysis (if so, one would have expected the rates to differ by 10−100-fold or more). Further, all of the mutants in this study exhibit retinal release E_a values that are quite similar. It is possible that the introduced mutations structurally perturb the protein enough to expedite retinal release (A295S) or slightly slow it (E122D). The Arrhenius plots

of retinal release rates illustrate that the slopes for most of the mutants are similar to that of WT, while their intercepts differ (Figure 5). We interpret this to mean that the slight structural perturbations that these mutants confer are generally entropic in nature (*52*). The exception is E122D which, judged by its slightly different slope, has enthalpic contributions as well. Additionally, since the rates of MII decay (which monitors Schiff base hydrolysis) differ among the various mutants, the E_a values for the overall process of retinal release are relatively similar. These data support the theory that chemical hydrolysis is the rate-limiting step in the retinal release pathway.

Functional Blue-Wavelength-Shifted Mutant. The information gleaned from the characterization and analysis of the individual blue-wavelength-shifting point mutations was used to construct a triple point mutant, T118A/E122D/A292S. In designing this mutant, we omitted mutant G90S (because of the perturbed photobleaching properties) and mutant A295S (because of the faster retinal release rate and minimal transducin activation). Our results suggest that mutant T118A/E122D/A292S confers a substantial blue-wavelength shift while retaining most of its structural stability and ability to activate transducin [note the normal photobleaching properties (Figure 6) and ability to activate transducin (Table 3)]. We propose mutant T118A/E122D/A292S will be useful in biophysical studies since the 47 nm blue shift allows the protein to tolerate yellow-orange light (~560 nm) at higher intensity than WT, which offers a practical advantage when handling the protein for techniques such as NMR and X-ray crystallography. Additionally, we have begun to use the T118A/E122D/A292S mutant in fluorescent spectroscopic studies. One of the difficulties of using fluorescent probes to study rhodopsin is the amount of spectral overlap of the fluorescent probes' emission with the dark and MII state of rhodopsin. While fluorescent probes that have little spectral overlap with rhodopsin exist, they are all large and bulky, potentially perturbing the protein domains into which they are introduced. The substantial blue-wavelength shift of mutant T118A/E122D/A292S will facilitate site-directed fluorescent labeling (SDFL) studies of rhodopsin by allowing the determination of the percent fluorescent change due to energy transfer from the fluorophore to the retinal in the dark and MII states. This will also enable the use of small fluorescent probes, such as those previously described (*26*). Studies of this nature are currently under way in our laboratory.

ACKNOWLEDGMENT

We thank Dr. J. Denu and Dr. H. P. Bächinger for helpful discussions regarding kinetics and thermodynamic analysis, and Dr. D. Oprian and members of the Farrens lab (T. Dunham, S. Mansoor, J. Fay, and Dr. B. Nauert) for critical reading of the manuscript.

REFERENCES

1. Fasick, J. I., Lee, N., and Oprian, D. D. (1999) *Biochemistry 38*, 11593−11596.
2. Merbs, S. L., and Nathans, J. (1993) *Photochem. Photobiol. 58*, 706−710.
3. Oprian, D. D., Asenjo, A. B., Lee, N., and Pelletier, S. L. (1991) *Biochemistry 30*, 11367−11372.
4. Khorana, H. G. (1992) *J. Biol. Chem. 267*, 1−4.
5. Helmreich, E. J., and Hofmann, K. P. (1996) *Biochim. Biophys. Acta 1286*, 285−322.
6. Sakmar, T. P. (1998) *Prog. Nucleic Acid Res. Mol. Biol. 59*, 1−34.
7. Wald, G. (1968) *Nature 219*, 800−807.
8. Hargrave, P. A., Hamm, H. E., and Hofmann, K. P. (1993) *BioEssays 15*, 43−50.
9. Nakanishi, K., Balogh-Nair, V., Arnaboldi, M., and Tsujimoto, M. (1980) *J. Am. Chem. Soc. 102*, 7947−7949.
10. Lin, S. W., Kochendoerfer, G. G., Carroll, K. S., Wang, D., Mathies, R. A., and Sakmar, T. P. (1998) *J. Biol. Chem. 273*, 24583−24591.
11. Asenjo, A. B., Rim, J., and Oprian, D. D. (1994) *Neuron 12*, 1131−1138.
12. Neitz, M., Neitz, J., and Jacobs, G. H. (1991) *Science 252*, 971−974.
13. Yokoyama, R., and Yokoyama, S. (1990) *Proc. Natl. Acad. Sci. U.S.A. 87*, 9315−9318.
14. Chan, T., Lee, M., and Sakmar, T. P. (1992) *J. Biol. Chem. 267*, 9478−9480.
15. Kochendoerfer, G. G., Wang, Z., Oprian, D. D., and Mathies, R. A. (1997) *Biochemistry 36*, 6577−6587.
16. Wang, Z., Asenjo, A. B., and Oprian, D. D. (1993) *Biochemistry 32*, 2125−2130.
17. Kleinschmidt, J., and Harosi, F. I. (1992) *Proc. Natl. Acad. Sci. U.S.A. 89*, 9181−9185.
18. Palczewski, K., Kumasaka, T., Hori, T., Behnke, C. A., Motoshima, H., Fox, B. A., Le Trong, I., Teller, D. C., Okada, T., Stenkamp, R. E., Yamamoto, M., and Miyano, M. (2000) *Science 289*, 739−745.
19. Baehr, W., Morita, E. A., Swanson, R. J., and Applebury, M. L. (1982) *J. Biol. Chem. 257*, 6452−6460.
20. Ferretti, L., Karnik, S. S., Khorana, H. G., Nassal, M., and Oprian, D. D. (1986) *Proc. Natl. Acad. Sci. U.S.A. 83*, 599−603.
21. Yang, K., Farrens, D. L., Hubbell, W. L., and Khorana, H. G. (1996) *Biochemistry 35*, 12464−12469.
22. Fong, T. M. (1999) in *Structure−Function Analysis Of G Protein-Coupled Receptors* (Wess, J., Ed.) pp 1−20, Wiley-Liss, New York.
23. Oprian, D. D., Molday, R. S., Kaufman, R. J., and Khorana, H. G. (1987) *Proc. Natl. Acad. Sci. U.S.A. 84*, 8874−8878.
24. Farrens, D. L., Altenbach, C., Yang, K., Hubbell, W. L., and Khorana, H. G. (1996) *Science 274*, 768−770.
25. Reeves, P. J., Hwa, J., and Khorana, H. G. (1999) *Proc. Natl. Acad. Sci. U.S.A. 96*, 1927−1931.
26. Dunham, T. D., and Farrens, D. L. (1999) *J. Biol. Chem. 274*, 1683−1690.
27. Wald, G. B., and Brown, P. K. (1953) *J. Gen. Physiol. 37*, 189−200.
28. Sakamoto, T., and Khorana, H. G. (1995) *Proc. Natl. Acad. Sci. U.S.A. 92*, 249−253.
29. Yang, K., Farrens, D. L., Altenbach, C., Farahbakhsh, Z. T., Hubbell, W. L., and Khorana, H. G. (1996) *Biochemistry 35*, 14040−14046.
30. Sakmar, T. P., Franke, R. R., and Khorana, H. G. (1989) *Proc. Natl. Acad. Sci. U.S.A. 86*, 8309−8313.
31. Farrens, D. L., and Khorana, H. G. (1995) *J. Biol. Chem. 270*, 5073−5076.
32. Fahmy, K., Zvyaga, T. A., Sakmar, T. P., and Siebert, F. (1996) *Biochemistry 35*, 15065−15073.
33. Phillips, W. J., and Cerione, R. A. (1988) *J. Biol. Chem. 263*, 15498−15505.
34. Rao, V. R., Cohen, G. B., and Oprian, D. D. (1994) *Nature 367*, 639−642.
35. Nakayama, T. A., and Khorana, H. G. (1991) *J. Biol. Chem. 266*, 4269−4275.
36. Fasick, J. I., and Robsinson, P. R. (1998) *Biochemistry 37*, 433−438.
37. Ridge, K. D., Bhattacharya, S., Nakayama, T. A., and Khorana, H. G. (1992) *J. Biol. Chem. 267*, 6770−6775.
38. Kochendoerfer, G. G., Lin, S. W., Sakmar, T. P., and Mathies, R. A. (1999) *Trends Biochem. Sci. 24*, 300−305.

39. Hofmann, K. P. (1986) *Photobiochem. Photobiophys. 13*, 309−338.
40. Lewis, J. W., and Kliger, D. S. (1992) *J. Bioenerg. Biomembr. 24*, 201−210.
41. Resek, J. F., Farahbakhsh, Z. T., Hubbell, W. L., and Khorana, H. G. (1993) *Biochemistry 32*, 12025−12032.
42. Imai, H., Kojima, D., Oura, T., Tachibanaki, S., Terakita, A., and Shichida, Y. (1997) *Proc. Natl. Acad. Sci. U.S.A. 94*, 2322−2326.
43. Fahmy, K., and Sakmar, T. P. (1993) *Biochemistry 32*, 7229−7236.
44. Zvyaga, T. A., Fahmy, K., Siebert, F., and Sakmar, T. P. (1996) *Biochemistry 35*, 7536−7545.
45. Vogel, R., Fan, G. B., Sheves, M., and Siebert, F. (2000) *Biochemistry 39*, 8895−8908.
46. Shieh, T., Han, M., Sakmar, T. P., and Smith, S. O. (1997) *J. Mol. Biol. 269*, 373−384.
47. Ganter, U. M., Schmid, E. D., Perez-Sala, D., Rando, R. R., and Siebert, F. (1989) *Biochemistry 28*, 5954−5962.
48. Meyer, C. K., Bohme, M., Ockenfels, A., Gartner, W., Hofmann, K. P., and Ernst, O. P. (2000) *J. Biol. Chem. 275*, 19713−19718.
49. Birge, R. R., Murray, L. P., Pierce, B. M., Akita, H., Balogh-Nair, V., Findsen, L. A., and Nakanishi, K. (1985) *Proc. Natl. Acad. Sci. U.S.A. 82*, 4117−4121.
50. Nagata, T., Terakita, A., Kandori, H., Kojima, D., Shichida, Y., and Maeda, A. (1997) *Biochemistry 36*, 6164−6170.
51. Cooper, A., Dixon, S., Nutley, M., and Robb, J. (1987) *J. Am. Chem. Soc. 109*, 7254−7263.
52. Jung, K. H., Spudich, E. N., Dag, P., and Spudich, J. L. (1999) *Biochemistry 38*, 13270−13274.

BI002937I